

1 September 17, 2020 KB

2 **Fixation and effective size in a haploid-diploid population with asexual reproduction**

3

4 ***Kazuhiro Bessho, **Sarah P. Otto**

5 * *Saitama Medical University, 38 Morohongo Moroyama-machi, Iruma-gun, Saitama 350-0495,*

6 *Japan*

7 ***Department of Zoology, The University of British Columbia, Vancouver, BC, V6T 1Z4,*

8 *Canada*

9 * *besshokazuhiro.reserch@gmail.com; (+81) 049-276-2030*

10 ** *otto@zoology.ubc.ca; (+1) 604-822-2778*

11

12 (first version in bioRxiv, 17, September, 2020)

13

14 **Keywords:** haploid-diploid life cycle, Wright-Fisher model, fixation probability, effective

15 population size, heteromorphic and isomorphic life cycle

16

17

18 **Abstract**

19 The majority of population genetic theory assumes fully haploid or diploid organisms
20 with obligate sexuality, despite complex life cycles with alternating generations being commonly
21 observed. To reveal how natural selection and genetic drift shape the evolution of haploid-diploid
22 populations, we analyze a stochastic genetic model for populations that consist of a mixture of
23 haploid and diploid individuals, allowing for asexual reproduction and niche separation between
24 haploid and diploid stages. Applying a diffusion approximation, we derive the fixation
25 probability and describe its dependence on the reproductive values of haploid and diploid stages,
26 which depend strongly on the extent of asexual reproduction in each phase and on the ecological
27 differences between them.

28

29 **1. Introduction**

30 Sexual reproduction in eukaryotes generally consists of an alternation of generations,
31 where meiosis halves the number of chromosomes to produce haploids and syngamy brings
32 together haploid gametes to produce diploids. The extent of development in each ploidy phase
33 varies substantially (Bell 1982; 1994). In diplontic organisms, at one extreme, development and
34 growth occur only in the diploid phase, as is observed in most animals. Haplontic organisms, at
35 the other extreme, undergo mitotic growth only in the haploid stage, as is seen in some green
36 algae. In between these extremes, many terrestrial plants, macroalgae, and fungi exhibit both
37 haploid and diploid growth (haploid-diploid life cycles). These stages are typically free living in
38 macroalgae, with either macroscopically similar (isomorphic) or distinct (heteromorphic) forms
39 in the haploid and diploid stage (Raper and Flexer 1970; Wilson 1981; Mable and Otto 1998;
40 Coelho 2007).

41 To explain variation in life cycles, several theoretical models have analyzed the
42 deterministic dynamics of a modifier allele that alters the time spent in haploid and diploid
43 phases (e.g., Perrot et al. 1991; Otto and Goldstein 1992; Goldstein 1992; Otto 1994; Orr and
44 Otto 1994; Jenkins and Kirkpatrick 1995; Otto and Marks 1996; Scott and Rescan 2017).
45 However, there are some gaps between these models and the complexities seen in many haploid-
46 diploid species. For example, these models often treat haploid and diploid individuals as
47 ecologically equivalent, despite the frequent observation of niche differences and seasonal shifts
48 in prevalence (e.g., Drew 1949; Slocum 1980; Dethier 1981). Most of these models also assume
49 obligate sexuality (but see Otto and Marks 1996), despite asexuality being frequently observed
50 among haploid-diploid species (“asexual looping”). Furthermore, while several models have
51 explored how haploid-diploid life cycles might evolve, the impact of haploid-diploid life cycles

52 on evolutionary processes remains underexplored (see, e.g., Bessho and Otto 2017 on the impact
53 on fixation probabilities and Immler et al. 2012 on the maintenance of variation).

54 Here we contribute to evolutionary theory for haploid-diploid populations by
55 calculating the fixation probability of mutations using a stochastic genetic model. This builds
56 upon our previous work (Bessho and Otto 2017) by accounting for asexual looping and niche
57 differences between ploidy phases, both of which are common in macroalgae (Bell 1982; de
58 Wreede and Klinger 1988; Hawkes 1990). Haploid and diploid phases often differ
59 physiologically, and even isomorphic haploids and diploids may differ ecologically (Hannach
60 and Santelices 1985; Destombe et al. 1993; Dyck and de Wreede 2006; Thornber et al., 2006;
61 Vieira et al. 2018). We therefore explore different forms of density dependence, acting either
62 globally on the total population size (as in Bessho and Otto 2017) or locally on the population
63 size of haploids and diploids separately (Figure 1). We show that the fate of a mutation depends
64 strongly on the reproductive values of haploids and diploids, which in turn depend on the extent
65 of asexual reproduction and ecological differences between the phases.

66

67 **2. Model**

68 In Bessho and Otto (2017), we calculated the fixation probabilities by tracking the
69 dynamics of a resident allele (R) and a mutant allele (M) in haploid and diploid individuals, using
70 both a Wright-Fisher and a Moran model. In that model, reproduction was obligately sexual,
71 individuals were ecologically equivalent, and the total population size was held constant (global
72 density dependence). Below, we calculate the fixation probability by first considering asexual
73 reproduction in each phase, assuming that haploids and diploids are ecologically equivalent
74 (global population regulation), and then determine how these results are affected by niche
75 differences (local population regulation that is ploidy specific).

76

77 2.1. Haploid-diploid Wright-Fisher model with global regulation and asexual looping

78 Let $X_{(GT)}(t)$ be a random variable that represents the number of individuals with
79 “genotype” (GT) at time t with resident (R) and mutant alleles (M), and let $x_{(GT)}(t)$ represent a
80 particular outcome of this random variable. In the global regulation model, we assume a constant
81 population, $x_R + x_M + x_{RR} + x_{RM} + x_{MM} = N_{tot}$, that is strictly regulated regardless of the
82 ploidy of the individuals.

83 The reproductive output and the degree of asexuality are characterized by $w_{(GT)}$ and
84 a_H for haploids [$(GT) = R$ or M] and $w_{(GT)}$ and a_D for diploids [$(GT) = RR, RM$, and MM].
85 Specifically, diploid individuals produce $(1 - a_D)w_{(GT)}$ haploid spores (sexual reproduction)
86 and $a_D w_{(GT)}$ diploid offspring (asexual loop). Similarly, haploids produce $(1 - a_H)w_{(GT)}/2$
87 female gametes (sexual reproduction) and $a_H w_{(GT)}$ haploid offspring (asexual loop), where we
88 assume that the species is monoecious and invests equal resources in male and female gametes.
89 During syngamy, we assume that male gametes are not limiting, that mating is random, and that
90 female gametes are successfully fertilized with male gametes, at a rate $f_{(GT)}$ [$(GT) = R$ or M],
91 becoming diploid zygotes. For clarity, we describe the model with non-overlapping generations,
92 although we note that overlapping generations can be considered by including surviving adults in
93 the counts of asexual offspring ($a_D w_{(GT)}$ and $a_H w_{(GT)}$).

94 We define the selection coefficient ($s_{(GT)}$) and the degree of dominance (h) acting upon
95 the mutant allele such that: $f_M = f_R(1 - s_M^f)$, $w_M = w_R(1 - s_M^w)$, $w_{RM} = w_{RR}(1 - s_{RM}^w)$,
96 $w_{MM} = w_{RR}(1 - s_{MM}^w)$, and $h = s_{RM}^w/s_{MM}^w$. To perform the diffusion approximation, we assume
97 that selection is weak, $s_M^f = \epsilon \tilde{s}_M^f$ and $s_{(GT)}^w = \epsilon \tilde{s}_{(GT)}^w$, where ϵ is a small parameter.

98

99 2.2. Haploid-diploid Wright-Fisher model with local regulation and asexual looping

100 We then consider the case where density dependence regulates haploid and diploid
101 populations separately, which may occur if they have different resource needs or utilize different
102 habitats or microhabitats (for short-hand, we refer to this case as “local regulation”). More
103 specifically, we assume that the population size of haploids and diploids is separately regulated
104 and remains constant N_H and N_D ($x_R + x_M = N_H$ and $x_{RR} + x_{RM} + x_{MM} = N_D$), respectively.
105 We set $N_H + N_D = N_{tot}$, $\hat{p}_H^L = N_H/N_{tot}$, and $\hat{p}_D^L = N_D/N_{tot}$, which will then allow us to
106 compare the results of local and global regulation. Holding population sizes constant is assumed
107 strictly for mathematical convenience but may be reasonable for populations whose sizes are
108 strongly regulated by the availability of appropriate habitat.

109

110 3. Fixation probability in a haploid-diploid population

111 3.1. Fixation probability in the global regulation model

112 The fixation probability in a haploid-diploid population can be derived using a diffusion
113 approximation (Bessho and Otto 2017), but doing so requires that we approximate the dynamics
114 to reduce the dimensionality from four variables ($x_R, x_M, x_{RR}, x_{RM}, x_{MM}$, which sum to N_{tot}) down
115 to one. We do so by using a separation of time scales, deriving the first and second moments of the
116 mutant allele frequency. Specifically, we transform the number of individuals of each genotype,
117 $x_{(GT)}$, into new variables that allow us to separate the slower evolutionary dynamics and the faster
118 ecological dynamics (Appendix A):

$$p_{ave} = c_H p_H + c_D p_D, \quad (1a)$$

$$\delta_p = p_D - p_H, \quad (1b)$$

$$\eta_{HW} = 1 - \frac{1}{2p_D(1-p_D)} \frac{x_{RM}}{x_{RR} + x_{RM} + x_{MM}}, \quad (1c)$$

$$\rho_H = \frac{x_R + x_M}{N_{tot}}, \quad (1d)$$

119 where p_{ave} indicates the average allele frequency of haploids and diploids weighted by the class
 120 reproductive values (c_H and c_D , where $c_H + c_D = 1$, see next paragraph), δ_p indicates the
 121 difference in allele frequencies between haploids and diploids, η_{HW} indicates the departure from
 122 the Hardy-Weinberg equilibrium in diploids, and ρ_H indicates the frequency of haploids in the
 123 population. Within these equations, the frequencies of mutant alleles in haploids and diploids are
 124 $p_H = x_M/(x_R + x_M)$ and $p_D = \left(\frac{x_{RM}}{2} + x_{MM}\right)/(x_{RR} + x_{RM} + x_{MM})$. As similar variables are
 125 used in the model with local population regulation, we use superscripts to indicate the form of
 126 population regulation (“*Model*” is G for global or L for local regulation).

127 The class reproductive values of haploids and diploids are defined as follows. In linear
 128 models, “reproductive value” is a measure of the expected fraction of the population in the long-
 129 term future that descends from an individual of a particular type (e.g., age or stage class). Class
 130 reproductive values, as defined by Taylor (1990) and Rousset (2004, p.153), scale these individual
 131 reproductive values up to the whole population of each class (i.e., the product of the individual
 132 reproductive values times the class size). In the models considered here, the dynamics are non-
 133 linear because of competition for resources (N_{tot}). Nevertheless, we can approximate reproductive
 134 values by assuming that the population is near equilibrium with only resident alleles and by holding
 135 the strength of competition constant (see Supplementary *Mathematica* file for all calculations).
 136 Doing so, we find that the class reproductive values of haploids and diploids, expressed as
 137 proportions that sum to one, are:

$$c_H^G = \frac{(1 - a_H) \frac{f_R}{2} w_R (\hat{\rho}_H^G)^2}{(1 - a_H) \frac{f_R}{2} w_R (\hat{\rho}_H^G)^2 + (1 - a_D) w_{RR} (\hat{\rho}_D^G)^2}, \quad (2a)$$

$$c_D^G = \frac{(1 - a_D)w_{RR}(\hat{\rho}_D^G)^2}{(1 - a_H)\frac{f_R}{2}w_R(\hat{\rho}_H^G)^2 + (1 - a_D)w_{RR}(\hat{\rho}_D^G)^2} \quad (2b)$$

138 where $\hat{\rho}_H^G = 1 - \hat{\rho}_D^G$ is the equilibrium frequency of haploids in the global model (Eq. A.4). As a
 139 special case of interest, when populations are purely sexual ($a_H = a_D = 0$), we can plug the
 140 equilibrium for $\hat{\rho}_H^G$ from Eq. (A.4) into (2) and show that $c_H^G = c_D^G = 1/2$.

141 As discussed in Appendix A (see also Bessho and Otto 2017), equations (2) provide the
 142 only weights that allow ecological and evolutionary time scales to be separated when calculating
 143 the average allele frequency in equation (1a), which is why we take that to be the evolutionarily
 144 relevant average. Although one might initially think that diploids should count twice as much
 145 because they contain two allele copies and that the evolutionarily relevant average allele frequency
 146 would depend on the population sizes of haploids and diploids, a strict alternation of generations
 147 ($a_H = a_D = 0$) ensures that haploids and diploids contribute equally to long-term future
 148 generations, so that their reproductive values are equal and the evolutionarily relevant average
 149 allele frequency is $p_{ave} = (1/2)p_H + (1/2)p_D$ (Bessho and Otto 2017).

150 As with our previous model, we can track the slow evolutionary dynamics for the
 151 expected change in average allele frequency p_{ave} under weak selection, once the fast ecological
 152 dynamics have stabilized, as which point we can show that there are similar allele frequencies in
 153 haploids and diploids ($\delta_p \approx 0$), diploids are approximately at Hardy-Weinberg equilibrium
 154 ($\eta_{HW} \approx 0$), and the ratio of haploids is similar among mutant and resident genotypes ($\rho_H \approx \hat{\rho}_H^G$)
 155 (Appendix A, File S1). Furthermore, to leading order, the second moment of change in allele
 156 frequency is equal to the neutral case and can be derived in the diffusion limit ($N_{tot} \rightarrow \infty$).

157 Given a single variable, p_{ave} , changing slowly over evolutionary time, we can then use
 158 standard diffusion methods to calculate the fixation probability of a mutation in a haploid-diploid
 159 population, $u(p_0^{Model})$, where “Model” is G for global and L for local (considered in the next

160 section). The diffusion is a function of the first and second moments of change in the mutant allele
 161 frequency, $m^{Model}(p_{ave})$ and $v^{Model}(p_{ave})$, both measured in time units of N_{tot} generations:

$$u(p_0^{Model}) = \frac{\int_0^{p_0^{Model}} \exp[-2Q^{Model}(p')] dp'}{\int_0^1 \exp[-2Q^{Model}(p')] dp'}, \quad (3a)$$

$$m^{Model}(p_{ave}) = \frac{N_{tot} p_{ave} (1 - p_{ave})}{2} [2s_{ave}^{Model} + 2c_D^{Model} p_{ave} (1 - 2h) s_{MM}^w], \quad (3b)$$

$$v^{Model}(p_{ave}) = \frac{p_{ave} (1 - p_{ave}) [(c_D^{Model})^2 \hat{\rho}_H^{Model} + (c_H^{Model})^2 (2\hat{\rho}_D^{Model})]}{\hat{\rho}_H^{Model} (2\hat{\rho}_D^{Model})}. \quad (3c)$$

162 where p_0^{Model} is the initial allele frequency of mutants (we focus on the case with a single initial
 163 mutant allele, $p_0^{Model} = 1/[N_{tot}(\hat{\rho}_H^{Model} + 2\hat{\rho}_D^{Model})]$) and $Q^{Model}(p) =$
 164 $\int (m^{Model}(p)/v^{Model}(p)) dp$. For the global regulation model, the average selection acting upon
 165 rare mutant alleles across haploid and diploid stages, s_{ave}^G , can be calculated from the first moment
 166 equation (Appendix 1) and equals:

$$s_{ave}^{Model} = c_H^{Model} s_M^w + c_D^{Model} s_{RM}^w + \phi^{Model} c_D^{Model} \frac{s_M^f}{2}, \quad (4a)$$

$$\phi^{Model} = \frac{(1 - a_H) \tilde{w}_R \hat{\rho}_H^{Model}}{(1 - a_H) \tilde{w}_R \hat{\rho}_H^{Model} + a_D w_{RR} \hat{\rho}_D^{Model}}. \quad (4b)$$

167 where $\tilde{w}_R = f_R w_R / 2$ is the fitness of haploids considering the cost of sex. As we will see later,
 168 this equation is valid for local regulation model. The term ϕ^{Model} indicates the fraction of the
 169 diploids in the next generation that come from the union of gametes rather than diploid asexual
 170 reproduction. With obligately sexual haploid-diploids ($a_H = a_D = 0$, where $c_H^{Model} = c_D^{Model} =$
 171 $1/2$ and $\phi^{Model} = 1$), these results coincide with those of Bessho and Otto (2017).

172

173 3.2. Fixation probability in the local regulation model

174 We next derive the fixation probability in a haploid-diploid population when density
 175 dependence regulates haploid and diploid populations separately (Figure 1b), by again applying a

176 transformation of variables and separation of time scales. For the local regulation model, the
 177 appropriate weights for the average allele frequency are similar to the global regulation model,
 178 where now the class reproductive values, expressed as proportions, are:

$$c_H^L = \frac{1 + \frac{a_H w_R \hat{\rho}_H^L}{(1 - a_D) w_{RR} \hat{\rho}_D^L}}{2 + \frac{a_H w_R \hat{\rho}_H^L}{(1 - a_D) w_{RR} \hat{\rho}_D^L} + \frac{2}{f_R} \frac{a_D w_{RR} \hat{\rho}_D^L}{(1 - a_H) w_R \hat{\rho}_H^L}}, \quad (5a)$$

$$c_D^L = \frac{1 + \frac{2}{f_R} \frac{a_D w_{RR} \hat{\rho}_D^L}{(1 - a_H) w_R \hat{\rho}_H^L}}{2 + \frac{a_H w_R \hat{\rho}_H^L}{(1 - a_D) w_{RR} \hat{\rho}_D^L} + \frac{2}{f_R} \frac{a_D w_{RR} \hat{\rho}_D^L}{(1 - a_H) w_R \hat{\rho}_H^L}}. \quad (5b)$$

179
 180 After applying a separation of time scales and conducting a diffusion approximation, we conclude
 181 that the solution for the fixation probability in a haploid-diploid population, Eqs. (3), remains valid
 182 for the local regulation model (Supplementary *Mathematica* file), with the average selection
 183 coefficient now being given by Eqs. (5).

184
 185 3.3. Effective genetic parameters

186 Using the first and second moments of change in allele frequency, we derive effective
 187 genetic parameters to compare our results to the dynamics found in the classical model for fully
 188 haploid or fully diploid organisms (Bessho and Otto 2017). More specifically, we define the
 189 effective selection coefficient (s_e), dominance coefficient (h_e), and effective population size (N_e)
 190 that would result in the same expected change in allele frequency and variance as in the classical
 191 diploid model of selection.

192 For selection, the diploid model is: $\Delta p_{ave} = s_e p_{ave} (1 - p_{ave}) [h_e + (1 - 2h_e) p_{ave}]$
 193 (Crow and Kimura 1970; Bessho and Otto 2017). Because this equation depends on the allele
 194 frequency in the same way as Eq. (3b), we can find the effective and dominance selection

195 coefficient from $\Delta p_{ave}/[p_{ave}(1-p_{ave})] = s_e h_e$ when $p_{ave} = 0$ and
 196 $\Delta p_{ave}/[p_{ave}(1-p_{ave})] = s_e(1-h_e)$ when $p_{ave} = 1$, yielding:

$$s_e^{Model} = 2s_{ave}^{Model} + 2\hat{c}_D^{Model} \frac{(1-2h)s_{MM}^w}{2}. \quad (6a)$$

$$h_e^{Model} = \frac{2s_{ave}^{Model}}{4s_{ave}^{Model} + 2\hat{c}_D^{Model}(1-2h)s_{MM}^w}. \quad (6b)$$

197 When the mutation is additive ($h = 1/2$), these effective parameters are $s_e^{Model} = 2s_{ave}^{Model}$ and
 198 $h_e^{Model} = 1/2$.

199 We next derive the variance effective population size by equating the one generation
 200 change in variance (Eq. 3c divided by the time scale, N_{tot}) to the variance in allele frequency
 201 expected in the classical Wright-Fisher model, $p_{ave}(1-p_{ave})/2N_e$ with N_e diploid individuals,
 202 obtaining:

$$N_e^{Model} = \frac{p_{ave}(1-p_{ave})}{2(v^{Model}/N_{tot})} = \frac{N_{tot} \hat{\rho}_H^{Model} \hat{\rho}_D^{Model}}{(c_D^{Model})^2 \hat{\rho}_H^{Model} + 2(c_H^{Model})^2 \hat{\rho}_D^{Model}}. \quad (7)$$

203 Plugging these effective parameters into the formula from the fixation probability in the
 204 classical diploid Wright-Fisher model (Kimura 1957; 1962; Crow and Kimura 1970, p. 427), the
 205 fixation probability in a haploid-diploid population given by Eq. 3a can be expressed as:

$$u(p_0^{Model}) = \frac{\int_0^{p_0^{Model}} \exp[-2N_e^{Model} s_e^{Model} \{(2h_e^{Model} - 1)p'(1-p') + p'\}] dp'}{\int_0^1 \exp[-2N_e^{Model} s_e^{Model} \{(2h_e^{Model} - 1)p'(1-p') + p'\}] dp'}. \quad (8)$$

206 Assuming an initially rare and additive mutation ($h = 1/2$) with weak positive selection in a large
 207 population ($s_e^{Model} N_e^{Model} p_0^{Model} \approx 0$ and $s_e^{Model} N_e^{Model} \gg 1$), we obtain the classic
 208 approximation, $u(p_0^{Model}) \approx 2s_e^{Model} N_e^{Model} p_0^{Model}$, which upon substituting from Eq. 7 yields:

$$u(p_0^{Model}) \approx \frac{2\hat{\rho}_H^{Model} \hat{\rho}_D^{Model}}{(\hat{\rho}_H^{Model} + 2\hat{\rho}_D^{Model}) \left[(c_D^{Model})^2 \hat{\rho}_H^{Model} + 2(c_H^{Model})^2 \hat{\rho}_D^{Model} \right]} 2s_{ave}^{Model}. \quad (9a)$$

209 For example, because haploids and diploids have the same reproductive values in the obligately
 210 sexual case ($\hat{c}_H^{Model} = \hat{c}_D^{Model} = 1/2$), we obtain:

$$u(p_0^{Model}) \approx \frac{8\hat{\rho}_H^{Model} \hat{\rho}_D^{Model}}{(\hat{\rho}_H^{Model} + 2\hat{\rho}_D^{Model})^2} 2s_{ave}^{Model} \quad (9b)$$

211 (Eq. 13a in Bessho and Otto 2017), or simply $u(p_0^{Model}) \approx 2s_{ave}^{Model}$ if haploid and diploid
212 population sizes are equal in terms of number of chromosomes ($\hat{\rho}_H^{Model} = 2/3$).

213 In the next three sections, we explore the implications of these results for the evolution
214 of haploid-diploid populations.

215

216 3.4. Effective selection in a haploid-diploid population

217 The strength of selection averaged across haploids and diploids, s_{ave}^{Model} , plays a key
218 role in the evolution of haploid-diploid populations. When a mutation is rare, both the rate of
219 change in allele frequency (Eq. 3b) and the approximate fixation probability (Eq. 10a) are
220 proportional to s_{ave}^{Model} . We thus begin by exploring how s_{ave}^{Model} varies as we alter the amount of
221 asexual reproduction in haploid and diploid phases. We focus on the case where the mutation does
222 not affect fertilization success ($s_M^f = 0$), so that the average selection becomes:

$$s_{ave}^{Model} = c_H^{Model} s_M^w + c_D^{Model} s_{RM}^w, \quad (10)$$

223 in both global and local regulation models (Eqs. (4) and (6)).

224 The relative evolutionary importance of selection in the haploid and diploid phases is
225 thus determined by the class reproductive values, c_H^{Model} and c_D^{Model} (where $c_H^{Model} +$
226 $c_D^{Model} = 1$). Figures 2 (global regulation) and 3 (local regulation) illustrate the proportional
227 reproductive value of haploids, c_H^{Model} , as a function of the degree of asexual reproduction in
228 haploids (x-axis) and diploids (ranging from 0.05 in red to 0.95 in blue). With global regulation,
229 the frequency of haploidy within the population, $\hat{\rho}_H^G$ (given by Eq. A.4), varies with the
230 parameters (see inset graphs in Figure 2), rising with the frequency of haploid asexuality (x-axis
231 in inset) but declining with more asexuality in diploids (from red to blue). By contrast, with local
232 regulation, the frequency of haploidy is held fixed by the strict density dependent competition that
233 we have assumed ($\hat{\rho}_H^L = 0.8$ in Figure 3(a)(b) and 0.3 in 3(c)(d)).

234 In the left panels, haploids have a higher fertility ($w_R/w_{RR} = 5$), leading to a higher
235 haploid reproductive value, c_H^{Model} , especially with local regulation when haploids are also more
236 common ($\hat{\rho}_H^L = 0.8$ in Figure 3a). In the right panels, diploids have a higher fertility ($w_{RR}/w_R =$
237 5), leading to a lower haploid reproductive value, especially when haploids are rare ($\hat{\rho}_H^L = 0.3$ in
238 Figure 3d).

239 When haploids are primarily sexual ($a_H \approx 0$), increasing asexuality of the haploid stage
240 typically causes the reproductive value of haploids to rise, unless diploids are fitter and more
241 frequent (Figure 3d and blue curves in Figure 2b). At the other extreme, the reproductive value of
242 haploids typically plummets to zero as haploid reproduction becomes primarily asexual ($a_H \approx 1$)
243 while diploids remain sexual, particularly with local regulation (Figure 3), because haploids then
244 act as a genetic “sink” contributing little to the diploid sub-population. This downward trend when
245 haploids are predominantly asexual is also seen with global regulation if diploids are more fit
246 (Figure 2b), except when the diploid population does not sustain itself and goes extinct, which
247 occurs when $a_D < 0.2$ and $a_H = 1$. The net result can thus be non-monotonic (purple curves
248 with $0.2 < a_D < 0.4$ in Figure 2b and Figure 3(a)(b)(c)).

249

250 3.4. Effective population size in a haploid-diploid population

251 We next consider the effective size of haploid-diploid populations with varying degrees
252 of asexuality. Figure 4 plots the effective population size (Eq. 8) relative to the total population
253 size, N_e^{Model}/N_{tot} , as a function of the frequency of haploids, $\hat{\rho}_H^{Model}$ (x-axis), and the class
254 reproductive values (with c_H^{Model} ranging from 0.05 in blue to 0.95 in red). As noted by Bessho
255 and Otto (2017), the effective population size is highest – and drift weakest – at intermediate
256 frequencies of haploids and diploids, which ensures the least sampling error as organisms alternate
257 generations.

258 When haploids and diploids have equal reproductive values, as in the fully sexual case
259 $(c_H^{Model} = c_D^{Model} = 1/2)$, the effective population size is maximized at $\hat{\rho}_H^{Model} \approx 0.586$. With
260 asexual reproduction, the peak shifts towards whichever ploidy level has the higher reproductive
261 value. For example, if haploids have a high reproductive value (red) then the effective population
262 size is maximized at a higher frequency of haploids, reducing the amount of genetic drift in that
263 phase. Although not illustrated, the peak shifts to $N_e^{Model} = \hat{\rho}_D^{Model} N_{tot}$ when future populations
264 descend only from diploids ($c_H^{Model} = 0$) and to $N_e^{Model} = (\hat{\rho}_H^{Model}/2) N_{tot}$ when future
265 populations descend only from haploids ($c_H^{Model} = 1$), effectively becoming diplontic or haplontic,
266 respectively (with the $1/2$ arising because haploids have half the number of chromosomes).

267 Of course, the reproductive values, as well as the frequency of haploids with global
268 population regulation ($\hat{\rho}_H^G$), depend in turn on the fitness parameters and the extent of asexuality,
269 as explored in the previous section. Figures 5 (global regulation) and 6 (local regulation) illustrate
270 the effective population size as a function of the frequency of haploid asexuality, a_H (x-axis), and
271 the frequency of diploid asexuality (a_D rising from red to blue), using the parameters in Figures 2
272 and 3, respectively. The trends are often non-monotonic, with N_e^{Model}/N_{tot} values varying
273 around $1/2$ when the parameter values are intermediate. The effective population size is often
274 higher when diploids rarely reproduce asexually (red) rather than when they frequently do (blue),
275 although there are exceptions (particularly when the fitness and frequency of diploids is high).

276

277 3.6. Fixation probability in a haploid-diploid population

278 We next compare the above results with numerical simulations estimating the fixation
279 probability of a newly arisen mutation in a haploid-diploid population. When simulating the global
280 regulation model, we assumed that the population has reached the demographic equilibrium,
281 $\hat{\rho}_H^G N_{tot}$ haploids and $\hat{\rho}_D^G N_{tot}$ diploids (see Appendix A). We then chose one resident allele R at

282 random and replaced it with a mutant allele M . After mutation, offspring were sampled from the
 283 parental generation according to a multinomial distribution with expected frequencies given by
 284 $x_{(GT)}$, repeating until the mutant allele fixed or was lost from the population. We estimated the
 285 fixation probability as the fraction of 10,000 replicate simulations leading to fixation.

286 We here consider the additive case ($h = 1/2$ and $h_e = 1/2$), where the fixation
 287 probability (Eq. 8) simplifies to:

$$u(p_0^{Model}) = \frac{\exp[-2p_0^{Model} N_e^{Model} s_e^{Model}] - 1}{\exp[-2N_e^{Model} s_e^{Model}] - 1} \quad (11)$$

288 and where $s_e^{Model} = 2 s_{ave}^{Model}$ (Eq. 6). Figure 7 plots the fixation probability as a function of the
 289 average selection pressure, s_{ave}^{Model} , when the reproductive values and chromosome numbers in
 290 haploids and diploids are equal ($c_H^{Model} = c_D^{Model}$ and $\hat{\rho}_H^{Model} = 2/3$) and $s_{ave}^{Model} = [(1/2)s_M^W +$
 291 $(1/2)s_{RM}^W]$. The diffusion Eq. (11) provides an excellent fit, as does the approximation Eq. (9b)
 292 for selection coefficients that are positive and not too weak. In this case, the results are the same
 293 with global and local population regulation (Fig. 7a and 7b, respectively) and are insensitive to
 294 how much selection occurs in the haploid or diploid phases (s_M^{Model} and s_{RM}^{Model} , respectively), as
 295 long as s_{ave}^{Model} is held constant (see additional simulations in Supplementary *Mathematica* file).
 296 As expected, the extent of selection in the haploid versus diploid phase matters more when the
 297 mutation is not additive ($h \neq 1/2$ and $h_e \neq 1/2$) (supplementary *Mathematica* file).

298 Next, we illustrate the approximate fixation probability, Eq. (9a), as a function of the
 299 degree of asexuality (a_H and a_D) when the population size is globally (Fig. 8) or locally (Fig. 9)
 300 regulated, assuming only selection in haploids or only in diploids. For example, with additive
 301 mutations, the fixation probability can be approximated as $u \approx 4c_H^{Model} N_e^{Model} p_0^{Model} s_M^W$ when
 302 selection occurs only in the haploid phase or $u \approx 4c_D^{Model} N_e^{Model} p_0^{Model} s_{RM}^W$ with selection only
 303 in the diploid phase, indicating that the fate of mutations depends as much on the strength of
 304 selection as on the reproductive value of the ploidy phase in which selection acts (as illustrated in

305 Fig. 2 and 3). Figures 8 (global) and 9 (local) illustrate how the fixation probability depends on the
306 various parameters in the model, particularly the amount of asexual reproduction in haploids (x-
307 axis) and diploids (a_D rising from red to blue). The trends can be understood by the combined
308 effects of the parameters on the reproductive value and the effective population size (e.g., Fig. 9(a)
309 is proportional to the product of Fig. 3(a) and Fig. 6(c)).

310

311 **4. Discussion**

312 Across the phylogenetic tree of life, organisms have diverse and complex reproductive
313 strategies (Bell 1982). Classical population genetic theory has, however, focused most on fully
314 haploid or diploid life cycles with obligate sexuality. In this article we develop a stochastic model
315 for the population genetics of haploid-diploid organisms considering demography, asexuality, and
316 habitat differentiation between haploid and diploid stages. Using a separation of time scales, we
317 derive a diffusion approximation for the change in allele frequency, allowing us to estimate the
318 fixation probability of new mutations, the effective strengths of selection and dominance, as well
319 as the effective population size of haploid-diploid populations.

320

321 5.1. Natural selection in a haploid-diploid population

322 Our results indicate that the strength of natural selection and the extent of genetic drift
323 depend strongly on the reproductive value of haploid versus diploid phases. In the simplest case,
324 when the effect of a mutation is weak, additive, positive, and absent in the gamete stage ($s_M^f = 0$),
325 the fixation probability is proportional to the effective strength of selection (Eq. 10), $s_e^{Model} =$
326 $2s_{ave}^{Model}$, which in turn is proportional to the amount of selection in and the reproductive value of
327 haploids and diploids (Eqs. 2, and 5).

328 These analytical results reveal some evolutionary principles for populations that undergo

329 an alternation of generations. One consequence is that the balance of opposing selection pressures
330 in haploids and diploids (Eqs. 4 and 6) depends not only on the selection coefficients, but also on
331 the relative reproductive values of haploids (c_H^{Model}) versus diploids (c_D^{Model}). Thus, the very
332 direction of evolution depends on the extent of asexuality in the two phases and the relative survival
333 and fertility of haploids versus diploids when there is “ploidy antagonistic selection” (Immler et
334 al. 2012).

335 The efficacy of selection to fine tune traits in haploids and diploids also depends on the
336 class reproductive values. For example, when the population is regulated by local density
337 dependence (i.e., the haploid and diploid phases are spatially or temporally distinct), higher
338 reproductive success in haploids increases the efficiency of haploid selection (compare Figure 3a
339 to 3b). However, when there is extremely rare sexuality in haploids (a_H near one), diploid
340 selection tends to be more effective because of increasing competition between offspring from
341 haploids. By contrast, the trends differ with global density dependence (e.g., species that are more
342 isomorphic with small ecological differences between stages). For example, the reproductive value
343 of haploids remains high even when they reproduce primarily asexually in the global regulation
344 model (see Figure 2 when a_H approaches one), because haploids then make up a larger proportion
345 of the total population size (see inset figures). Thus, whether selection is effective in the haploid
346 phase when that phase mainly reproduces asexually is quite sensitive to the nature of competition.

347 Our work can also be useful in the design of field studies and the interpretation of data
348 for species that alternate generations. To understand the efficiency of selection on haploid and
349 diploid phases, we not only need data about the fraction of haploids and diploids and their fertility
350 and mortality (e.g., Thornber and Gains 2004; Vieira et al., 2018a; Vieira et al. 2018b), but we also
351 need to know about the extent of asexuality in each phase and whether they compete for common
352 or different resources.

353

354 5.2. Genetic drift and effective size

355 The impact of random genetic drift on the genetic diversity of haploid-diploid population
356 depends on the effective population size (Eq. 7). As we had found previously in a haploid-diploid
357 model with obligate sexuality (Bessho and Otto 2017, pp. 431), the effective population size with
358 asexuality is generally smaller than the total number of individuals and again depends strongly on
359 the reproductive value of each phase (Figures 4-6). With obligate sexuality, the reproductive values
360 of haploids and diploids are equal, and the effective population size is maximized (drift minimized)
361 when haploids comprise $2/3$ of the population, making the number of chromosomes equal between
362 haploids and diploids. Asexual reproduction, however, causes the reproductive value of haploids
363 and diploids to differ (Eqs. 2 and 5). Consequently, drift is lessened if the phase with the higher
364 reproductive value is more common (see shifts in peaks in Figure 4).

365

366 5.3. "Ploidally-structured" population

367 The key role that reproductive values play in this work is analogous to the role that patch
368 dynamics play in two-patch models of evolution. In a spatially structured population, subdivided
369 local populations are genetically connected by migration. A haploid-diploid system can be seen as
370 being ploidally structured, where gene flow describes the movement of alleles through sexual
371 reproduction, with meiosis causing flow to haploidy and syngamy flow to diploidy. We note that
372 our research reveals that all qualitative results are equally accurate for evolution in a two-patch
373 system (see Supplementary *Mathematica* File). For example, fixation probability strongly depends
374 on class reproductive values of each patch.

375 This analogy suggests an interesting idea: complex reproductive systems can be
376 considered and analyzed using the tools of metapopulation theory. For example, many eukaryotes

377 including terrestrial plants, insects, and fishes, often exhibit ploidy variation, including polyploid
378 members (Otto and Whitton 2000; Comai 2005). In such species, individuals characterized by
379 different numbers of chromosomes coexist, with complex reproductive relationships causing gene
380 flow between them (Ramsey and Schemske 1998). Similarly, social insects often exhibit complex
381 sex determination systems linked with ploidy levels (haplodiploidy).

382 Our research suggests that these ploidally-structured populations can be fruitfully treated
383 as metapopulations. Selection and drift in populations with diploids, triploids, and tetraploids can,
384 for example, be considered as a three-patch model. In this system, we conjecture that the average
385 strength of selection that is evolutionarily relevant would be the mean selection coefficient in each
386 ploidy class, weighted by its class reproductive value, with additional terms coming from
387 reproductive interactions (akin to the term of s_M^f in Eqs. 4).

388 Many evolutionary aspects of haploid-diploid populations remain to be investigated. One
389 avenue that we are exploring is how model parameters can be estimated from field data. For
390 example, the analogy between spatially and ploidally structured population suggests that genetic
391 differences between haploids and diploid can be used to estimate gene flow between them (i.e.,
392 rates of sex), akin to using F_{st} to inform estimates of migration (e.g., Slatkin 1987). Another fruitful
393 avenue for further work is to determine how fluctuations in population size affect the effective
394 population size of species that alternate generations. In classical population genetics theory, such
395 fluctuations can be captured by using the harmonic mean population in place of the total population
396 size (Karlin 1968). It is unclear, however, whether the same is true in haploid-diploid populations.
397 Can the harmonic total population size simply replace N_{tot} in the global model of population
398 regulation? Similarly, can the harmonic population sizes of haploids and diploids replace N_H and
399 N_D with local regulation? The answer is unclear because population size fluctuations perturb the
400 fast ecological dynamics away from the steady state (especially $\hat{\rho}_H^{Model}$), and the impact of these

401 perturbations on selection and drift is unknown. Further research is needed to clarify evolutionary
 402 processes in the wide variety of species that alternate generations.

403

404 **Acknowledgements**

405 We here thank Alireza Ghaseminejad for help in developing our manuscript. This project was
 406 funded by a Grand-in-Aid from a Japan Society for the Promotion of Science (JSPS) to KB
 407 (16J05204) and by a Discovery grant from the Natural Sciences and Engineering Research Council
 408 of Canada (NSERC RGPIN-2016-03711) to S.P.O.

409

410 **Appendix A. Fixation probability in a haploid-diploid Wright-Fisher model using a** 411 **diffusion approximation**

412 A.1. Equilibrium with global regulation

413 We derive the fixation probability in a haploid-diploid population using a diffusion
 414 approximation (e.g., Bessho and Otto 2017). We first derive the stable equilibrium in the global
 415 regulation model, allowing for asexual reproduction in each phase. In the Wright-Fisher model,
 416 all individuals reproduce and then the parents die (non-overlapping generations). Let $b_{(GT)}$
 417 represent the number of reproductive cells of each type in the next generation:

$$b_R = (1 - a_D)w_{RR}x_{RR} + (1 - a_D)\frac{w_{RM}x_{RM}}{2} + a_H w_R x_R, \quad (\text{A.1a})$$

$$b_M = (1 - a_D)\frac{w_{RM}x_{RM}}{2} + (1 - a_D)w_{MM}x_{MM} + a_H w_M x_M, \quad (\text{A.1b})$$

$$b_{RR} = (1 - a_H)\frac{f_R}{2}\frac{w_R^2 x_R^2}{w_R x_R + w_M x_M} + a_D w_{RR} x_{RR}, \quad (\text{A.1c})$$

$$b_{RM} = (1 - a_H)\frac{f_R + f_M}{2}\frac{w_R w_M x_R x_M}{w_R x_R + w_M x_M} + a_D w_{RM} x_{RM}, \quad (\text{A.1d})$$

$$b_{MM} = (1 - a_H)\frac{f_M}{2}\frac{w_M^2 x_M^2}{w_R x_R + w_M x_M} + a_D w_{MM} x_{MM}. \quad (\text{A.1e})$$

418 The probability that a reproductive cell of genotype (GT) is sampled from the offspring produced
 419 by the previous generation of adults is

$$q_{(GT)} = \frac{b_{(GT)}}{b_R + b_M + b_{RR} + b_{RM} + b_{MM}}. \quad (\text{A.2})$$

420 Therefore, the composition of offspring in the next generation is given by the multinomial
 421 distribution, sampling N_{tot} individuals in proportion to Eq. (A2). Using Eq. (A1) and (A2), we
 422 describe the conditional expectation of change in the number of individuals of genotype (GT),
 423 $\Delta X_{(GT)}(t) = X_{(GT)}(t+1) - X_{(GT)}(t)$, as

$$E[\Delta X_{(GT)}(t) | \vec{X}(t) = \vec{x}] = N_{tot} q_{(GT)} - x_{(GT)}, \quad (\text{A.3})$$

424 where $E[\Delta F(X_{(GT)}(t)) | \vec{X}(t) = \vec{x}]$ is the conditional expected value for change in the function
 425 F of the random variable given that $\vec{X}(t) = (X_R(t) \ X_M(t) \ X_{RR}(t) \ X_{RM}(t) \ X_{MM}(t))^T$
 426 equals $\vec{x} = (x_R \ x_M \ x_{RR} \ x_{RM} \ x_{MM})^T$.

427 To simplify this fully stochastic system, we assume that the resident population is large
 428 and treat demographic changes deterministically prior to the appearance of the mutation.
 429 Considering the dynamics of the resident population, we then find the equilibrium of these
 430 dynamical equations by solving $N_{tot} q_R - \hat{x}_R = 0$ and $N_{tot} q_{RR} - \hat{x}_{RR} = 0$ ($\hat{x}_R + \hat{x}_{RR} = N_{tot}$).
 431 Setting $\hat{x}_R = \hat{\rho}_H^G N_{tot}$ and $\hat{x}_{RR} = \hat{\rho}_D^G N_{tot}$, the fraction of haploids $\hat{\rho}_H^G$ (and diploids $\hat{\rho}_D^G = 1 -$
 432 $\hat{\rho}_H^G$) at equilibrium becomes,

$$\hat{\rho}_H^G = \frac{a_H w_R + a_D w_{RR} - 2w_{RR} + \sqrt{4(1 - a_H)(1 - a_D)\tilde{w}_R w_{RR} + (a_H w_R - a_D w_{RR})^2}}{2[a_H w_R + (1 - a_H)\tilde{w}_R - w_{RR}]}, \quad (\text{A.4})$$

433 where $\tilde{w}_R = f_R w_R / 2$ is the fitness of haploids considering the cost of sex (see Supplementary
 434 *Mathematica* file for the step-by-step derivation). We note that, when the fertility of haploids is
 435 much greater than that of diploids ($w_R \gg w_{RR}$), the frequency of haploids in a population
 436 approaches $a_H / \{a_H + [(1 - a_H)f_R / 2]\}$, which is less than one because sexual reproduction of
 437 the haploids produces diploids (the $(1 - a_H)f_R / 2$ term). Conversely, when the fertility of

438 diploids is much greater than haploids ($w_R \ll w_{RR}$), the frequency of haploids approaches 1 –
 439 a_D , the rate at which diploids undergo meiosis.

440

441 A.2. First moment of change in allele frequency

442 To derive the first moment of change in allele frequency, $m^{Model}(p_{ave})$, we apply a
 443 separation of time scales (e.g., Nagylaki 1976; Otto and Day 2007; Bessho and Otto 2017).

444 Details of the calculation are represented in the Supplementary *Mathematica* file. We first
 445 transform the expected change in the number of individuals of each type (five variables that sum
 446 to N_{tot}) into the expected change in a new set of four variables, $\theta \in \{p_{ave}, \delta_p, \eta_{HW}, \rho_H\}$,

447 described by the functions:

$$E[\Delta\theta|\vec{X}(t) = \vec{x}] = f_{\theta}^{Model}(\epsilon, p_{ave}, \vec{\theta}), \quad (\text{A.5})$$

448 where $\vec{\theta} = (\delta_p, \eta_{HW}, \rho_H)$ and ϵ is proportional to the selection coefficients and assumed small
 449 (the functions f are given explicitly in the Supplementary *Mathematica* file). With local
 450 regulation, ρ_H is assumed fixed at N_H/N_{tot} and dropped from the variable set, θ .

451 To constant order (setting the small changes due to selection to zero, $\epsilon \rightarrow 0$), the fast
 452 ecological dynamics of the system are described by: $f_{\theta}^{Model}(0, p_{ave}, \vec{\theta})$. This system of
 453 equations rapidly approaches a steady state found by solving $f_{\theta}^{Model}(0, p_{ave}, \vec{\theta}) = 0$, which
 454 gives $\bar{\delta}_p = \bar{\eta}_{HW} = 0$, and $\bar{\rho}_H = \hat{\rho}_H^G$ (Eq. A.4). To this order, the steady state change in allele
 455 frequency is zero, $f_{p_{ave}}^{Model}(0, p_{ave}, \vec{\theta}) = 0$. We then describe slower changes, including changes
 456 in allele frequency due to selection, by describing the deviations that occur around this steady
 457 state. Specifically, to order ϵ , the variables are allowed to deviate from the steady state by $\delta_p =$
 458 $\tilde{\delta}_p\epsilon$, $\eta_{HW} = \tilde{\eta}_{HW}\epsilon$, and $\rho_H = \hat{\rho}_H^G + \tilde{\rho}_H\epsilon$, and the dynamics $f_{\theta}^{Model}(\epsilon, p_{ave}, \vec{\theta})$ are then
 459 approximated using a Taylor series expansion. Defining the average allele frequency by
 460 combining haploid and diploid populations using an arbitrary weighting, $p_{ave} = \omega p_H +$

461 $(1 - \omega)p_D$, we show in the Supplementary *Mathematica* file that setting the weights proportional
 462 to the class reproductive values (given by Eq. (2) with global regulation and Eq. (5) with local
 463 regulation) is the only choice that separates evolutionary change in p_{ave} from changes in the
 464 other variables to order ϵ . Defining the average allele frequency in this way (Eq. 1a) and taking
 465 the Taylor series, the change in allele frequency becomes:

$$\begin{aligned} \mathbb{E}[\Delta p_{ave} | \vec{X}(t) = \vec{x}] &\approx M^{Model}(p_{ave}) & (A.6) \\ &= \frac{p_{ave}(1 - p_{ave})}{2} \left[2s_{ave}^{Model} + 2c_D^{Model} p_{ave}(1 - 2h)s_{MM}^w \right]. \end{aligned}$$

466

467 A.3. Second moment of change in average allele frequency

468 We next derive the second moment of change in average allele frequency in a haploid-
 469 diploid population with asexuality. We again assume that the population size is very large, that
 470 selection is very weak, and that the system has approached the steady state in $(\delta_p, \eta_{HW}, \rho_H)$,
 471 ignoring deviations that are of $O(\epsilon)$. Because selection is assumed weak, the second moment is
 472 well approximated by that of the neutral model (to constant order, $\epsilon \rightarrow 0$).

473 Under these assumptions, the fraction of haploids in a population is relatively fixed in
 474 both the global and local regulation models, and we can sample the haploid offspring according
 475 to a binomial distribution, with expectation and variance: $\mathbb{E}[X_M | \vec{X}(t) = \vec{x}] = q_M N_H$ and
 476 $\text{Var}[X_M | \vec{X}(t) = \vec{x}] = q_M(1 - q_M)N_H$ where $q_M = b_M/(b_R + b_M)$. To simplify the equation,
 477 we set $\mathbb{E}[X_{(GT)} | \vec{X}(t) = \vec{x}] = m_{(GT)}$ and $\text{Var}[X_{(GT)} | \vec{X}(t) = \vec{x}] = v_{(GT)}$, finding that:

$$\mathbb{E}[\Delta X_M | \vec{X}(t) = \vec{x}] = m_M - x_M, \quad (A.7a)$$

$$\mathbb{E}[(\Delta X_M)^2 | \vec{X}(t) = \vec{x}] = v_M + m_M^2 - 2m_M x_M + x_M^2. \quad (A.7b)$$

478 In terms of allele frequencies (rather than numbers), we have the first and second moments for

479 the haploid offspring population, $E\left[\frac{\Delta X_M}{N_H} \mid \vec{X}(t) = \vec{x}\right] = \frac{1}{N_H} E[\Delta X_M \mid \vec{X}(t) = \vec{x}]$ and

480 $E\left[\left(\frac{\Delta X_M}{N_H}\right)^2 \mid \vec{X}(t) = \vec{x}\right] = \frac{1}{N_H^2} E[(\Delta X_M)^2 \mid \vec{X}(t) = \vec{x}].$

481 Similarly, the diploid offspring are sampled according to a trinomial distribution, with

482 expectation, variance, and covariance: $m_{(GT)} = q_{(GT)}N_D$, $v_{(GT)} = q_{(GT)}(1 - q_{(GT)})N_D$, and

483 $\text{Cov}[X_{RM}, X_{MM} \mid \vec{X}(t) = \vec{x}] = q_{RM}q_{MM}N_D$, where $q_{(GT)} = b_{(GT)}/(b_{RR} + b_{RM} + b_{MM})$. To derive

484 the moments of the allele frequency in diploids, we define, $y_M = (x_{RM}/2) + x_{MM}$ and $Y_M =$

485 $(X_{RM}/2) + X_{MM}$. The moments of random variable Y are then:

$$E[Y_M \mid \vec{X}(t) = \vec{x}] = \frac{m_{RM}}{2} + m_{MM}, \quad (\text{A.8a})$$

$$E[Y_M^2 \mid \vec{X}(t) = \vec{x}] = \frac{v_{RM} + m_{RM}^2}{4} + (\text{Cov}[X_{RM}, X_{MM} \mid \vec{X}(t) = \vec{x}] + m_{RM}m_{MM}) + (v_{MM} + m_{MM}^2), \quad (\text{A.8b})$$

$$E[\Delta Y_M \mid \vec{X}(t) = \vec{x}] = \frac{E[\Delta X_{RM} \mid \vec{X}(t) = \vec{x}]}{2} + E[\Delta X_{MM} \mid \vec{X}(t) = \vec{x}] - y_M, \quad (\text{A.8c})$$

$$E[(\Delta Y_M)^2 \mid \vec{X}(t) = \vec{x}] = E[Y_M^2 \mid \vec{X}(t) = \vec{x}] - 2E[Y_M \mid \vec{X}(t) = \vec{x}]y_M + y_M^2. \quad (\text{A.8d})$$

486 To consider the change in average allele frequency across the entire population, we

487 define $Z_M = c_H^{Model} \frac{X_M}{N_H} + c_D^{Model} \frac{Y_M}{N_D}$ and consider the expectation of change in this random

488 variable. Plugging in Eqs. (7a), (7b), (8c), and (8d), we have

$$E[(\Delta Z_M)^2 \mid \vec{X}(t) = \vec{x}] = \frac{p_{ave}(1 - p_{ave}) \left[(c_D^{Model})^2 \hat{\rho}_H^{Model} + (c_H^{Model})^2 (2\hat{\rho}_D^{Model}) \right]}{\hat{\rho}_H^{Model} (2\hat{\rho}_D^{Model}) N_{tot}}. \quad (\text{A.9})$$

489 After transforming time scales using the variable $\tau = t/N_{tot}$ and defining $P(\tau) = Z(N_{tot}\tau)$,

490 we have the diffusion coefficient $v^{Model}(p_{ave}) = \lim_{N_{tot} \rightarrow \infty} E\left[\frac{(P(\tau+\Delta\tau) - P(\tau))^2}{\Delta\tau}\right]$ by taking the limit

491 $N_{tot} \rightarrow \infty$, giving Eq. (3c). Similarly, we derive the drift coefficient using Eq. (A6) ($m^{Model} =$

492 $M^{Model}N_{tot}$), giving Eq. (3b).

493

494 **References**

- 495 Bell, G. 1982. The Masterpiece of Nature: The Genetics and Evolution of Sexuality. University
496 of California Press. Berkeley, CA.
- 497 Bell, G., 1994. The comparative biology of the alternation of generations. Lectures on
498 mathematics in the life sciences 25, 1–26.
- 499 Bessho, K., Otto, S. P. 2017. Fixation probability in a haploid-diploid population. *Genetics* 205,
500 421-440.
- 501 Comai, L. 2005. The advantages and disadvantages of being polyploid. *Nature Reviews Genetics*
502 6, 836-846.
- 503 Coelho, S. M., Peters, A. F., Charrier, B., Roze, D., Destombe, C., Valero, M., Cock, J. M., 2007.
504 Complex life cycles of multicellular eukaryotes: new approaches based on the use of
505 model organisms. *Gene* 406, 152–170.
- 506 Crow, J. F., Kimura, M. (1970). An introduction to population genetics theory. The Blackburn
507 Press, New Jersey.
- 508 Deithier, M. N. (1981). Heteromorphic algal life histories: The seasonal pattern and response to
509 herbivory of the brown crust, *Ralfsia californica*. *Oecologia* 49, 333-339.
- 510 Destombe, C., Godin, J., Nocher, M., Richerd, S., Valero, M. (1993). Differences in response
511 between haploid and diploid isomorphic phases of *Gracilaria verrucosa* (Rhodophyta:
512 Gigartinales) exposed to artificial environmental conditions. *Hydrobiologia* 260/261, 131-
513 137.
- 514 De Wreede, R. E., Klinger, T. 1988. Reproductive strategies in algae. *Plant reproductive ecology:*
515 *Patterns and strategies*, 267-284.
- 516 Drew, K. M. (1949). Conchocelis-phase in the life-history of *Porphyra umbilicalis* (L.) Kütz.
517 *Nature* 164, 748-749.
- 518 Dyck, L. J., De Wreede, R. E. (2006). Seasonal and spatial patterns of population density in the
519 marine macroalga *Mazzaella splendens* (Gigartinales, Rhodophyta). *Phycological*
520 *Research*, 54(1), 21-31.
- 521 Goldstein, D. B. 1992. Heterozygote advantage and the evolution of dominant diploid phase.
522 *Genetics* 132, 1195–1198.
- 523 Hages, J. S., Otto, S. P. 1999. Ecology and the evolution of biphasic life cycles. *The American*
524 *Naturalist* 154, 306–330.
- 525 Hannach, G., Santelices, B. 1985. Ecological differences between the isomorphic reproductive
526 phases of two species of *Iridaea* (Rhodophyta: Gigartinales). *Marine Ecology Progress*
527 *Series* 22, 291–303.
- 528 Hawkes, M. W. 1990. Reproductive strategies. *Biology of the red algae*, 455-476.

- 529 Immler, S., G. Arnqvist, and S. P. Otto. 2012. Ploidally antagonistic selection maintains stable
530 genetic polymorphism. *66*:55–65.
- 531 Jenkins, C. D., Kirkpatrick, M., 1995. Deleterious mutation and the evolution of genetic life
532 cycles. *Evolution*, 512–520.
- 533 Karlin, S. 1968. Rates of approach to homozygosity for finite stochastic models with variable
534 population size. *The American Naturalist* 102, 443-455.
- 535 Kimura, M., 1957. Some problems of stochastic processes in genetics. *The Annals of*
536 *Mathematical Statistics*, 882-901.
- 537 Kimura, M., 1962. On the probability of fixation of mutant genes in a population. *Genetics* 47,
538 713.
- 539 Mable, K. B., Otto, P. S., 1998. The evolution of life cycles with haploid and diploid phases.
540 *BioEssays* 20, 453–462.
- 541 Nagylaki, T., 1976. The evolution of one-and two-locus systems. *Genetics* 83, 583-600.
- 542 Orr, H. A., Otto, S. P. 1994. Does diploidy increase the rate of adaptation? *Genetics* 136, 1475–
543 1480.
- 544 Otto, S., Goldstein, D., 1992. Recombination and the evolution of diploidy. *Genetics* 131, 745–
545 751.
- 546 Otto, S., 1994. The role of deleterious and beneficial mutations in the evolution of ploidy levels.
547 *Lectures on Mathematica in the Life Sciences* 25, 69–98.
- 548 Otto, S. P., Marks, J. C. 1996. Mating system and the evolutionary transition between haploidy
549 and diploidy. *Biological Journal of the Linnean Society* 57, 197-218.
- 550 Otto, S. P., Day, T., 2007. A biologist's guide to mathematical modeling in ecology and
551 evolution. Princeton University Press.
- 552 Otto, S. P., Whitton, J. 2000. Polyploid incidence and evolution. *Annu. Rev. Genet.* 34, 401-437.
- 553 Perrot, V., Richerd, S., Valéro, M., 1991. Transition from haploidy to diploidy. *Nature* 351, 315–
554 317.
- 555 Ramsey, J., Schemske, D. W. 1998. Pathways, mechanisms, and rates of polyploid formation in
556 flowering plants. *Annual reviews of Ecology and Systematics* 29: 467-501.
- 557 Raper, J. R., Flexer, A. S. (1970). The road to diploidy with emphasis on a detour. In *Symp. Soc.*
558 *Gen. Microbiol* (Vol. 20, pp. 401-432).
- 559 Rousset, F. (2004). Genetic structure and selection in subdivided populations. Princeton
560 University Press, New Jersey.
- 561 Scott, M. F., Rescan, M. 2016. Evolution of haploid-diploid life cycles when haploid and diploid
562 fitnesses are not equal. *Evolution* 71, 215–226.
- 563 Slatkin, M. 1987. Gene flow and the geographic struture of natural populations. *Science New*
564 *Series* 236: 787-792.

- 565 Slocum C. J. 1980. Differential susceptibility to grazers in two phases of an intertidal alga:
566 Advantages of heteromorphic generations. *Journal of Experimental Marine Biology and*
567 *Ecology* 46, 99-110.
- 568 Taylor, P. D. 1980. Allele-Frequency Change in a Class-Structured Population. *The American*
569 *Naturalist* 135, 95-106.
- 570 Thornber, C. S., Gains, S. D. 2004. Population demographics in species with biphasic life cycle.
571 *Ecology* 85, 1661-1674.
- 572 Thornber, C., Stachowicz, J. J., Gains, S. 2006. Tissue type matters: selective herbivory on
573 different life history stages of an isomorphic alga. *Ecology* 87, 2255-2263.
- 574 Vieira, V. M. N. C. S., Engelen, A. H., Huanel, O. R., Guillemin, M. 2018a. Haploid females in
575 the isomorphic biphasic life-cycle of *Gracilaria chilensis* excel in survival. *BMC*
576 *Evolutionary Biology* 18:174.
- 577 Vieira, V. M. N. C. S., Engelen, A. H., Huanel, O. R., Guillemin, M. 2018b. Differentiation of
578 haploid and diploid fertilities in *Gracilaria chilensis* affect ploidy ratio. *BMC*
579 *Evolutionary Biology* 18:183.
- 580 Willson, M. F. 1981. On the evolution of complex life cycles in plants: a review and an
581 ecological perspective. *Annals of the Missouri Botanical Garden* 68, 275-300.

582

583 **Figure Captions**

584 Fig. 1. An illustration of the haploid-diploid models. (a) In the global regulation model, both
585 haploids and diploids occupy the same habitat and density dependence holds the total population
586 size N_{tot} constant. (b) In the local regulation model, each ploidy stage occupies a different
587 habit, therefore density dependence regulates the population size of haploids (N_H) and diploids
588 (N_D) separately.

589

590 Fig. 2. Class reproductive value of haploids in the global regulation model, c_H^G . Curves show c_H^G
591 as a function of the degree of haploid asexuality, a_H (x-axis), with the degree of diploid
592 asexuality ranging in color from $a_D = 0.05$ (red) to 0.95 (blue) in increments of 0.05. Other
593 parameters are set as: (a) $f_R = 0.5$, $w_R = 5000$, $w_{RR} = 1000$, (b) $f_R = 0.5$, $w_R = 1000$,
594 $w_{RR} = 5000$. The resulting frequency of haploids, $\hat{\rho}_H^G$ (Eq. A.4), is shown in the inset plots.

595
596 Fig. 3. Proportional reproductive value of haploids in the local regulation model, c_H^L . Parameters
597 are the same as Fig. 2, except that haploids are held fixed at a frequency of (a)(b) $\hat{\rho}_H^L = 0.8$ or
598 (c)(d) $\hat{\rho}_H^L = 0.3$. We consider the case when (a)(c) haploid fitness parameter is larger than
599 diploid $w_R = 5000$, $w_{RR} = 1000$ ($w_H > w_D$), and when (b)(d) diploid fitness parameter is
600 larger than haploid $w_R = 1000$, $w_{RR} = 5000$ ($w_H < w_D$).

601
602 Fig. 4. The effective population size of a haploid-diploid population. The relative effective
603 population size over the total population size (N_e^{Model}/N_{tot} , Eq. 7) is shown as a function of the
604 frequency of haploids ($\hat{\rho}_H^{Model}$, x-axis), when the haploid reproductive value (c_H^{Model}) varies from
605 0.05 (blue) to 0.95 (red) in increments of 0.05. This figure applies to both global and local
606 regulation models.

607
608 Fig. 5. The effective population size of a haploid-diploid population in the global regulation
609 model as a function of the degree of asexuality, a_H and a_D . Parameters are the same as in Fig. 2
610 and determine the relative class reproductive values (c_H^G) and fraction of haploids ($\hat{\rho}_H^G$) according
611 to Eqs. (2a) and (A.4).

612
613 Fig. 6. The effective population size of a haploid-diploid population in the local regulation
614 model. Parameters are the same as in Fig. 3 and determine the relative class reproductive values
615 (c_H^L) by Eqs. (5). The frequencies of haploids are held fixed at a frequency of (a)(b) $\hat{\rho}_H^L = 0.9$,
616 (c)(d) $\hat{\rho}_H^L = 0.8$, (e)(f) $\hat{\rho}_H^L = 0.6$, or (g)(h) $\hat{\rho}_H^L = 0.3$.

617

618 Fig. 7. Fixation probability given the average strength of selection, s_{ave}^{Model} , for global (a) and
619 local (b) regulation models. The solid curve gives the analytical result from the diffusion
620 approximation (Eq. (11)) and the dashed curve gives the linear approximation (Eq. (9b)). Black
621 dots indicate the fixation probability estimated from 10000 numerical simulations with 95% CI
622 (Wilson score interval for binomial). Parameters: $N_{tot} = 90$, $N_H = 60$, $N_D = 30$, $f_R = 0.5$,
623 $w_R = w_{RR} = 1000$, $a_H = a_D = 0.1$, $h = 0.5$, $s_M^f = 0$, $s_M^w = s_{RM}^w = s_{ave}^{Model}$, such that the
624 fraction of haploids in the resident population is $\hat{\rho}_H^{Model} = 2/3$ and class reproductive values
625 are equal $c_H^{Model} = c_D^{Model} = 1/2$. Holding $s_{ave}^{Model} = 1/2(s_M^w + s_{RM}^w)$ constant, similar results
626 are obtained for a range of different choices of s_M^w and s_{RM}^w (see supplementary *Mathematica*
627 file).

628
629 Fig. 8. The fixation probability in a haploid-diploid population in the global regulation model.
630 Curves gives the linear approximation for the fixation probability (Eq. (9a)). Parameters are the
631 same as in Fig. 2. Selection acts only in the haploid or diploid phase, with selection coefficients
632 set as $s_M^w = 0.02$ for haploid selection (a)(b) and $s_{RM}^w = 0.02$ for diploid selection (c)(d).

633
634 Fig. 9. The fixation probability in a haploid-diploid population in the local regulation model.
635 Curves gives the linear approximation for the fixation probability (Eq. (9a)). Parameters are the
636 same as in Fig. 3 and Fig. 8. The frequency of haploids is held fixed at (a)(b)(e)(f) $\hat{\rho}_H^L = 0.8$,
637 (c)(d)(g)(h) $\hat{\rho}_H^L = 0.3$. Fitness of haploids is higher than diploids in panels (a)(c)(e)(g) ($w_H >$
638 w_D), and the opposite condition is considered in panels (b)(d)(f)(h) ($w_H < w_D$). Selection only
639 occurs in the haploid (a)(b)(c)(d) or diploid stage (e)(f)(g)(h).

640

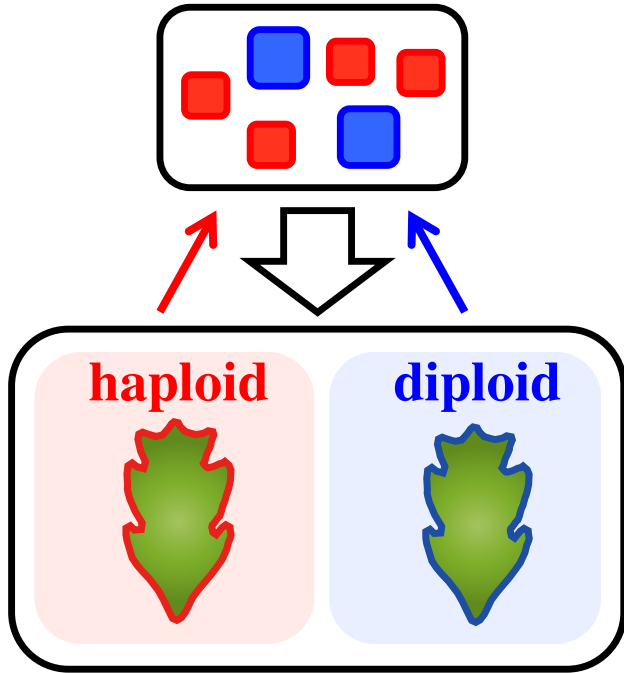
641 **Supporting information**

642 S1. Supplementary *Mathematica* file.

Figure 1

(a)

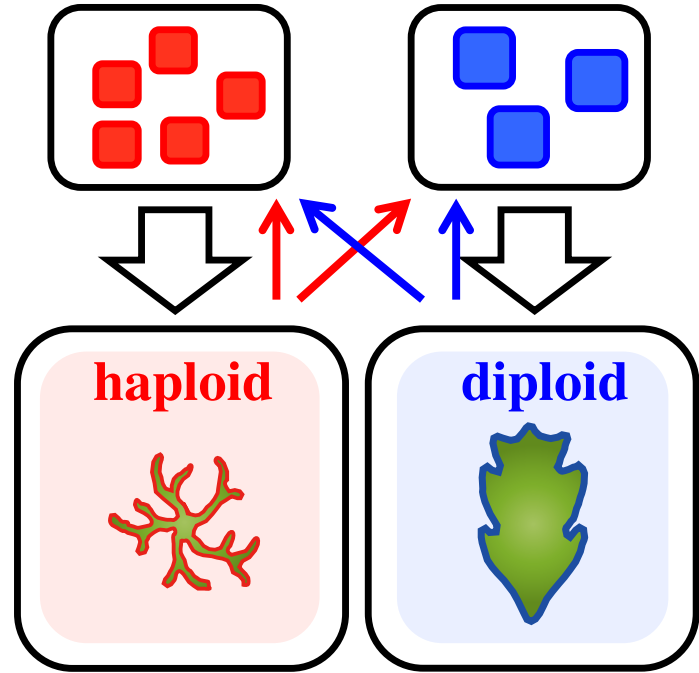
Global regulation



Total population size: N_{tot}

(b)

Local regulation



N_{H}

N_{D}

Figure 2

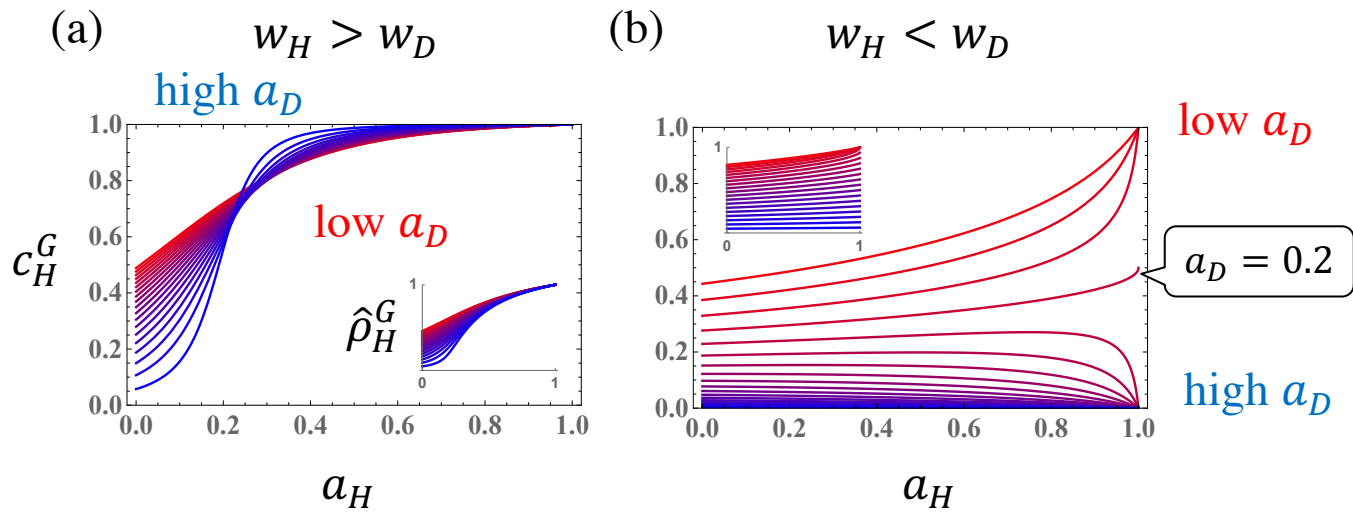
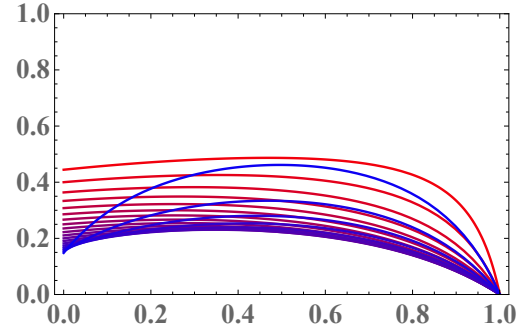
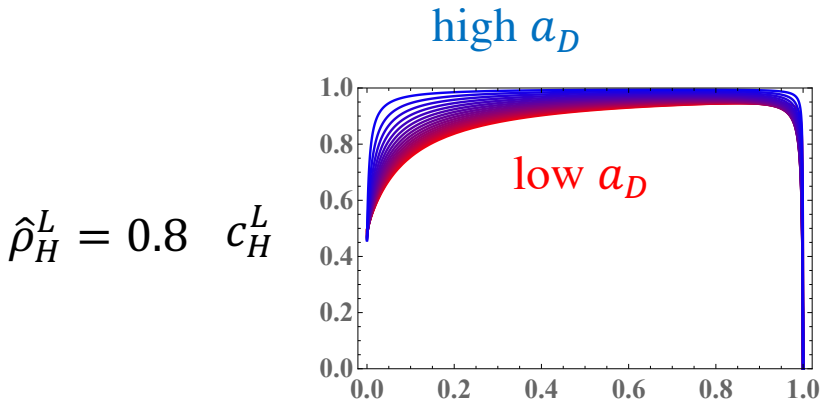


Figure 3

(a) $w_H > w_D$

(b) $w_H < w_D$



(c)

(d)

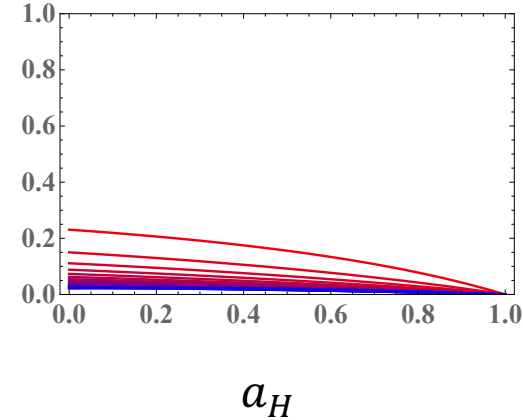
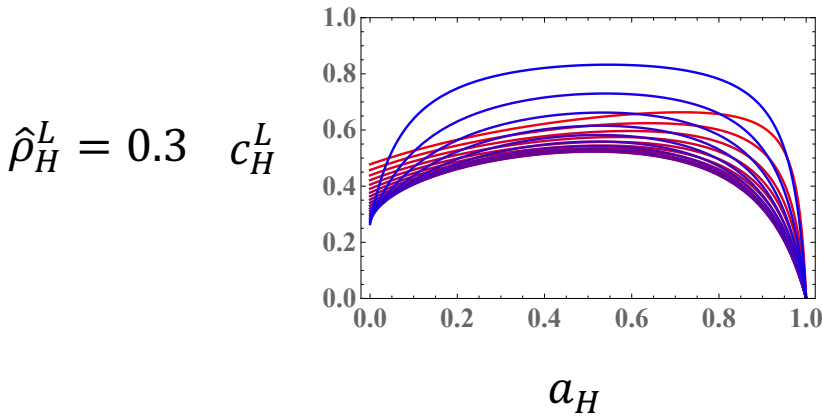


Figure 4

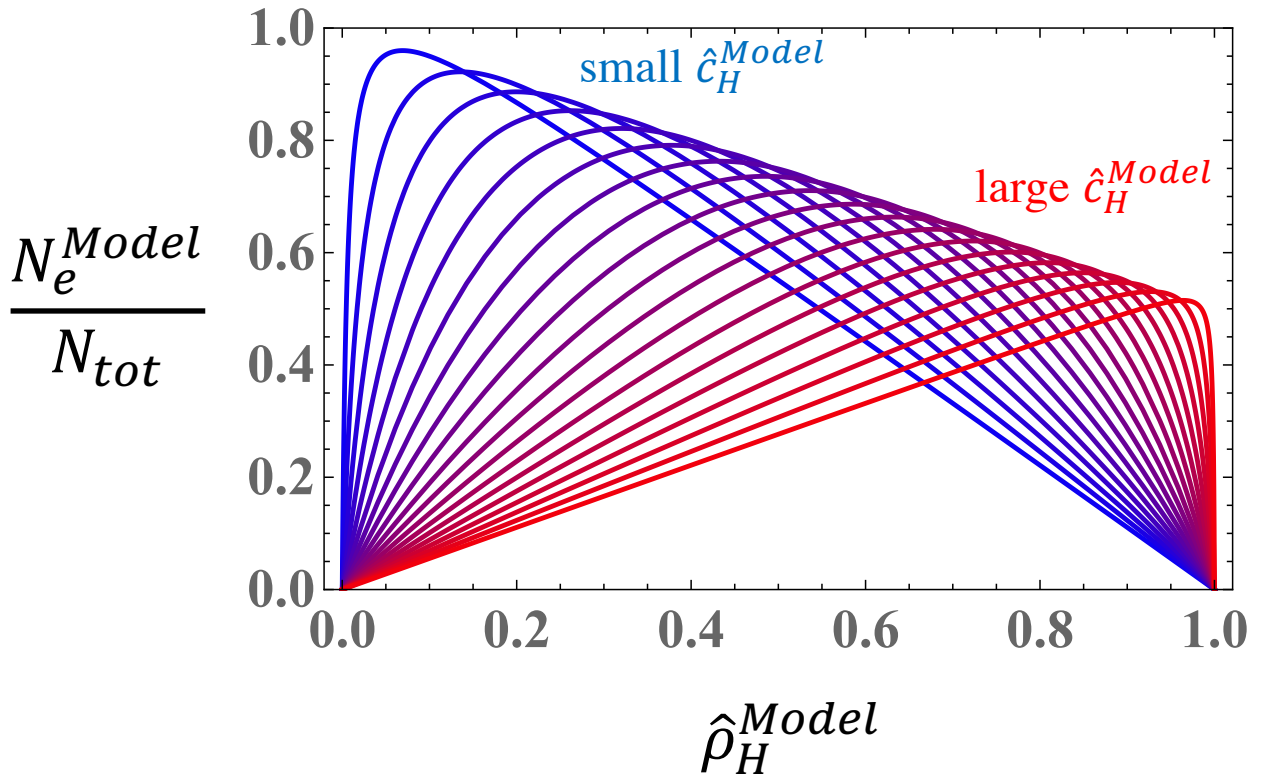


Figure 5

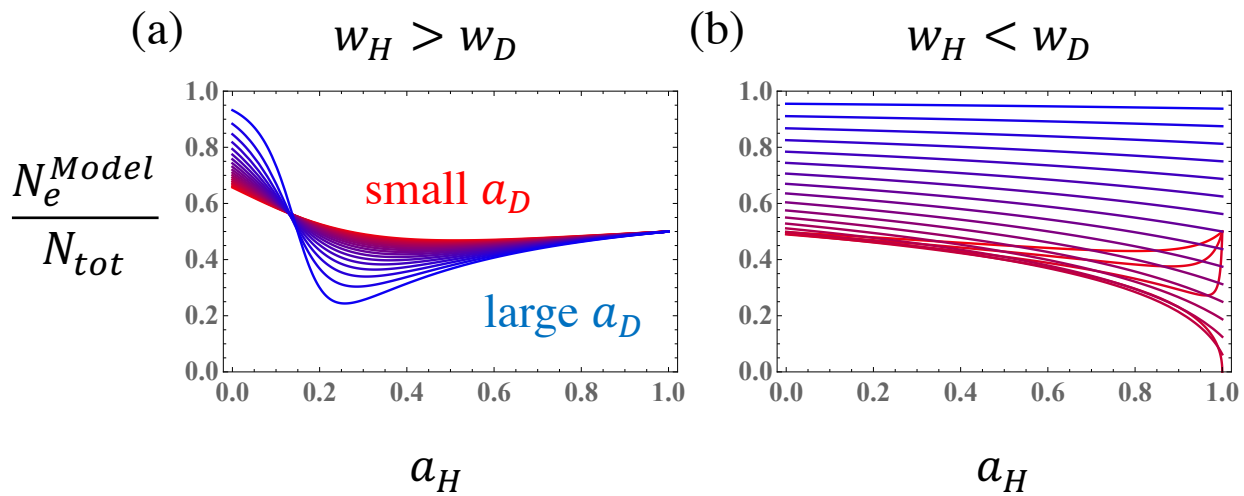


Figure 6

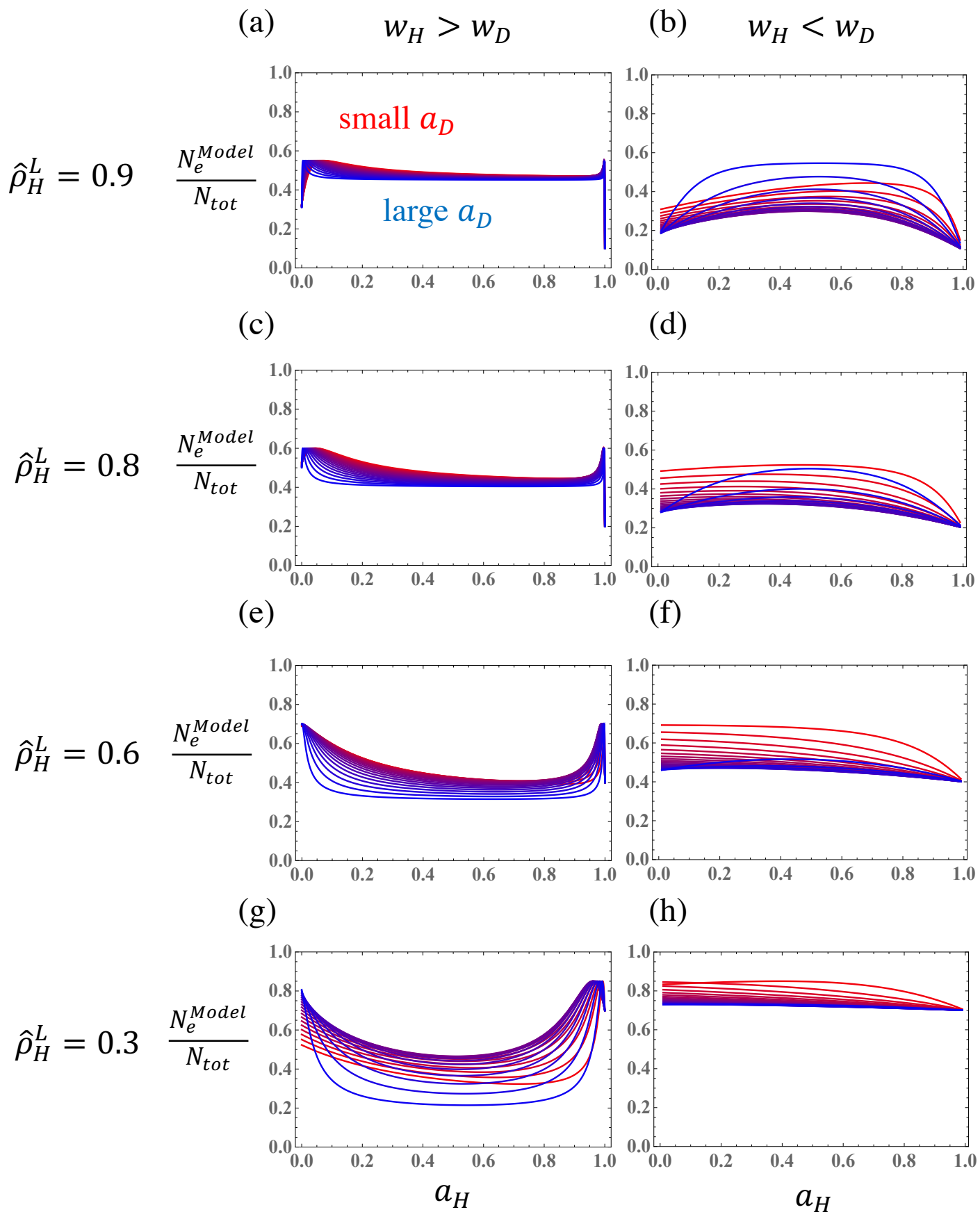
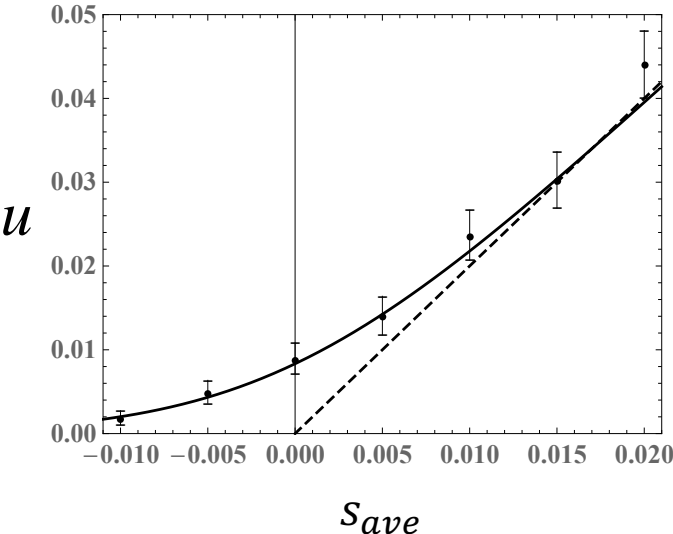


Figure 7

(a) global regulation



(b) local regulation

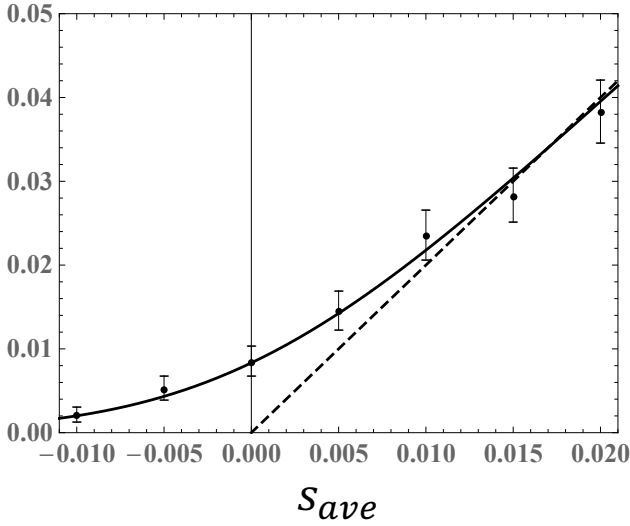


Figure 8

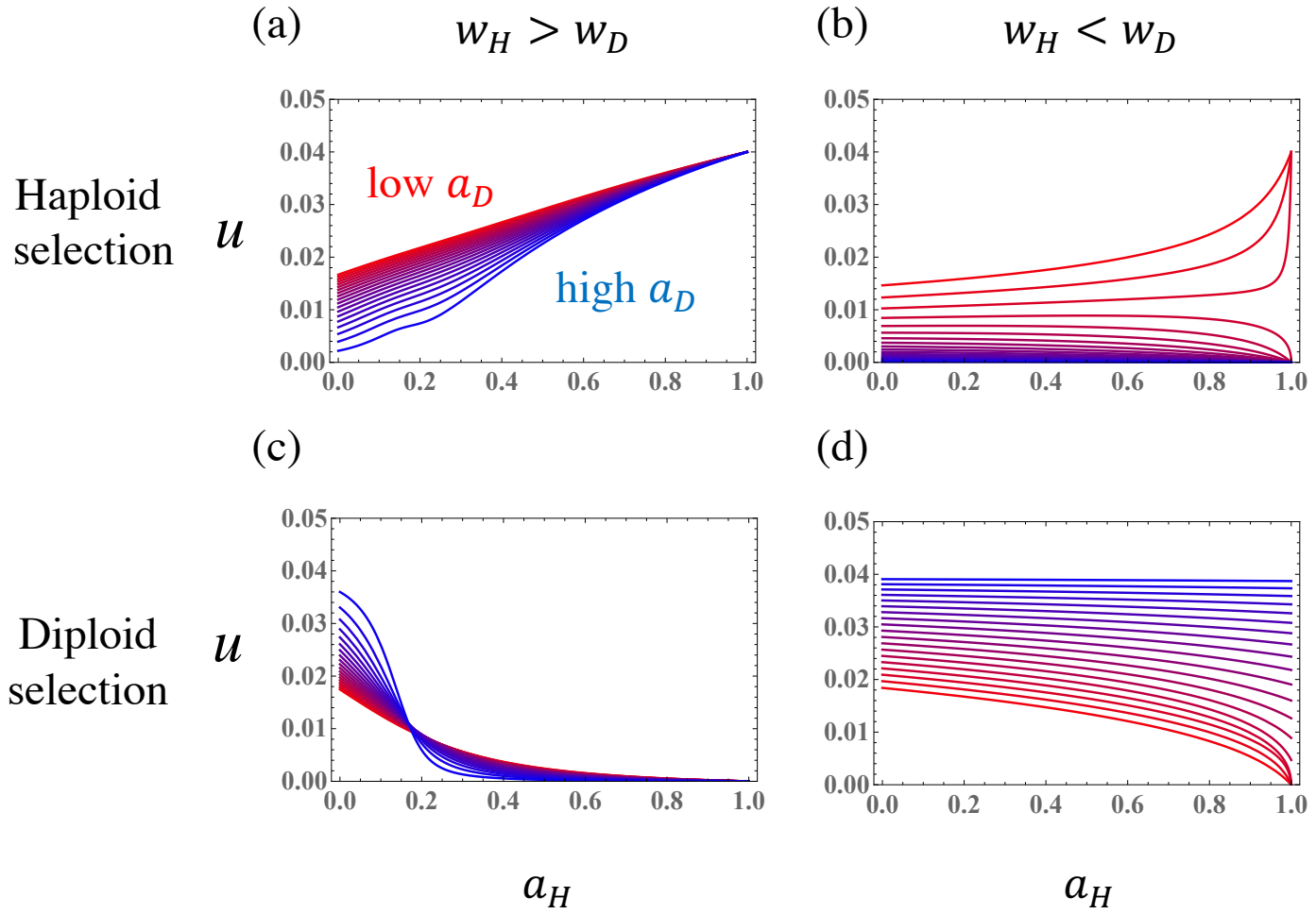


Figure 9

